ISSN: 0128-7680
Pertanika J. Sci. & Technol. Supplement 9(2): 107-115 (2001)

An Examination of Dynamic Stall Vortex Inception on a Finite Wing

Antonella Ferrecchia, Frank N. Coton & Roderick A. McD. Galbraith
Department of Aerospace Engineering, University of Glasgow, UK

ABSTRACT

In the present study, the behaviour of the vorticity flux on a wing of NACA 0015 cross-section was analysed for ramp-up motion over a range of dimensionless pitch rates. The variations in the vorticity flux were examined as a means to identify the role of the vorticity leaving the boundary layer in the initiation, development and growth of the dynamic stall vortex. It has been found that there are two main sources of bipolar vorticity located within the first 3% of the chord at all spanwise stations on the wing. These sources move and change strength as the wing is pitched through the incidence range. One factor that influences their behaviour is the reduced pitch rate and this effect is discussed. Further, it is shown that there is an apparent link between the negative source of vorticity and the first observable manifestation of the dynamic stall vortex on the pressure distribution near the mid-span.

Keywords: Dynamic Stall Vortex Fuception, Fiurtewing

INTRODUCTION

Dynamic stall has been extensively investigated because of its historical importance in helicopter applications. Consequently, a large body of literature on dynamic stall exists particularly in relation to rotorcraft applications; the phenomenon also occurs on compressor blades in turbomachinery and on wind turbines used to generate electricity. When an aerofoil is pitched through and beyond the incidence of static stall at a sufficiently high pitch rate, the resulting series of events is often termed dynamic stall. It is characterised by a significant lift overshoot, followed by a sudden loss of lift and a major surge in pitching moment. Carr, (1977), presented a detailed description of the events that contribute to this phenomenon. Firstly, as the angle of attack increases beyond the static stall angle, the flow around the oscillating aerofoil stays thin and essentially in viscid in nature. This delays the forward movement of trailing edge separation and extends the linear portion of the lift curve often up to and beyond the static stalling angle. Eventually, however, the boundary layer on the surface of the aerofoil shows symptoms of flow reversal, and this flow reversal spreads from the trailing edge toward the leading edge as the angle of attack continues to increase. At an angle which depends on many parameters, including aerofoil shape, pitch rate, frequency, Reynolds number and Mach number, the viscous flow no longer remains thin and attached, and a very strong vortical flow develops. This vortex begins near the leading edge of the aerofoil, grows in size, and then moves down the aerofoil, inducing strong pitching moment effects on the aerofoil. The increase in maximum lift, delay of stall, creation of the dynamic stall vortex, and major pitching moment variations are all typical of dynamic stall as observed on both helicopters and fixed wing aircraft.

Despite numerous research studies into the phenomenon of dynamic stall, the physical mechanisms that play fundamental roles in the initiation, development, growth, movement and detachment of the dynamic stall vortex are still not understood completely. In addition, the behaviour of the flow in the early stages of the inception of the vortex need to be examined carefully, and the mechanisms responsible for this evolution process need to be well understood. This paper focuses on the initiation of the dynamic

stall vortex by analysis of surface pressure measurements at the leading edge of a pitching rectangular wing. Several methods have been proposed to identify vortex inception on the basis of pressure measurements. Possibly the most straight forward of these involves the examination of individual pressure traces at a given chordal location to determine any sudden changes in the temporal pressure gradient. This allows the response, called Cp deviation, associated with the vortex formation to be isolated (Rosenhead 1963). This approach, however, requires prior knowledge of the location of vortex formation and may, therefore, be subjective. Possibly a more appropriate indicator of vortex inception may be forthcoming from a study of the behaviour of vorticity flux in the vicinity of the leading edge.

In this paper, a technique, based on the analysis of vorticity flux, is presented that allows vortex formation at the mid span of a finite wing to be identified. It is shown that the results obtained in this way compare well with the earliest occurrence of Cp deviation at the mid-span. In this way, the concept of vorticity flux is shown to be a potential indicator of vortex inception.

EXPERIMENTAL METHODS

The tests, which provided data for the present work, were carried out in the University of Glasgow wind tunnel which is a low speed closed-return type. The wing model was located horizontally in its 2.13 x 1.62 metre octagonal working section and supported on three struts. These were connected to the main support structure and a hydraulic actuation mechanism which was situated below the tunnel. Movement of the model was produced by displacement of the two rear struts and the model was pivoted about the quarter chord position on a tool steel shaft connected to the front support via two self aligning bearings.

The test model was a straight wing with a NACA 0015 cross-section. The wing had simple solids of revolution at its tips, Fig. 1. Because the lift behaviour at low aspect ratios is quite different from that at high aspect ratios, particularly when the aspect ratio is less than 2.0, the aspect ratio of this model was chosen as 3.0 to avoid strong three dimensional effects at the mid span in steady flow. In order to diminish the effect of upwash on the angle attack near the wing tips of the model and to reduce the blockage affect to minimum, the model size was carefully determined. The final overall dimensions were 126cm x 42cm which resulted in a variation of model blockage from a minimum of 2.6% to a maximum of 11.35% (not including the faring of struts) and a model span to tunnel width ratio of 0.592. According to previous studies of the blockage effect for 2D dynamic stall testing, these dimensions were considered acceptable. The model was constructed with an aluminium framework of ribs and stringers and an outer epoxy glass fibre skin.

To log the data, 192 pressure transducers were surface mounted within the model predominantly to the starboard side. There were six chordal distributions at various spanwise locations, each of which had 30 transducers. In the region of the tip, additional transducers were placed between the above mentioned sections to provide a better assessment of the tip vortex movement and structure. Moreover, to check on the overall symmetry of the flow, two transducers were placed on the left side of the wing in corresponding positions to their counterparts on the starboard side. All pressure transducers were of Kulite differential type CJQH-187 with one side of the pressure diaphragm open to the ambient pressure outside the wind tunnel via tubing. The signals from all of the transducers were taken to a specially designed signal conditioning unit of modular construction with each module containing its own control board. The data

acquisition was carried out by a PC microcomputer, configured with a 486 processor and interfaced with proprietary BE256 modules which provided the necessary analogue to digital conversion. At present, the system has 200 channels, each of which is capable of sampling to a maximum rate of 50KHz, giving an overall sampling rate of 10MHz. The reference dynamic pressure in the wind tunnel working section was determined by measuring the difference between the static pressure in the working section, upstream of the leading edge of the model, and the static pressure in the settling chamber. The pressure tapings were connected to a FURNESS FC012 micromanometer that provided an analogue signal suitable for the data acquisition unit.

Four particular types of test were considered in the full study. These were static tests, ramp up tests, ramp down tests and sinusoidal tests. In all cases, the model was rotated about its quarter chord axis to achieve the desired motion type. The data presented here are restricted to ramp up motions were the linear pitch rate is greater than 200 degrees/second. During a ramp test, the straight wing was rotated over a pre-set arc at a constant pitch rate. The ramp motion was repeated several times at each pitch rate and data from 4 cycles of motion were recorded. Previous experience has shown that there exists minor random differences in data from cycle to cycle for dynamic tests and that the salient features are highlighted by the averaging process. For this reason, the data presented in this report are the average of 4 cycles of 8000 samples. In all cases the wind tunnel velocity was around 50m/s.

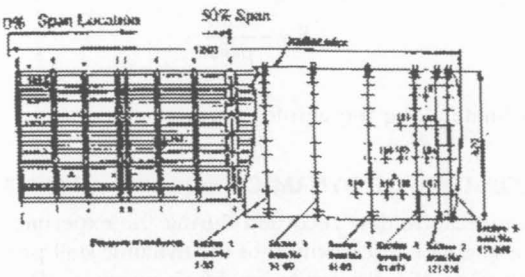

Fig. 1. Wing model with transducer distribution

VORTICITY FLUX

The role of vorticity, defined as the curl of velocity vector, in better understanding various fluid dynamic phenomena, is well established. Lighthill, in his introduction to boundary layer theory, provided an extensive description of vorticity dynamics in a variety of flows by using vorticity as the primitive variable for theoretical considerations. He was also the first to introduce the concept of Vorticity Flux density, S, and to point out the significance of solid boundaries as distributed sources and sinks of vorticity.

The motion of a surface and the flow events within the viscous region are strongly coupled; the unsteady separation process and the events of stall are strongly affected by the vorticity generated at the wall. In their review paper, Reynolds and Carr, showed that, for both steady and unsteady flows, the rate of vorticity flux is determined by the vorticity gradient of the boundary layer. Using span decomposition, the momentum equation along the surface provides a direct expression for the viscous vorticity flux:

$$S = -\frac{\partial U_2}{\partial t} - \frac{1}{\rho}\frac{\partial p}{\partial x} - V\omega_z \qquad (1)$$

where y is the normal to the surface, x is the coordinate along the surface, U_s is the surface tangential speed and V is the transpiration velocity flux at the rigid surface. The vorticity flux, S, may be expressed as

$$S = -\nu \frac{\partial \omega_z}{\partial y} \tag{2}$$

On the right hand side of Eqn. (1), the individual terms are the Surface Acceleration, Pressure Gradient and Transpiration respectively. The Vorticity Flux on the left hand side represents the flow of total vorticity out from the solid surface per unit area per unit time. The Surface Acceleration term represents the generation of vorticity in the Stokes layer due to acceleration of an infinite plate when the fluid is at rest. The Pressure Gradient term is the main source of vorticity in boundary layers. It is the source for vorticity generated at a surface at rest when the fluid above it is accelerated. The transpiration term is a source of vorticity when a fluid is sucked through a porous surface. On a curved surface Eqn. (1) is not exact, but for high Reynolds number it is still good approximation. It follows from Eqn. (1) that for constant motion of an aerofoil, and in the absence of transpiration, the flux of vorticity from the aerofoil surface is given by

$$S = -\frac{1}{\rho} \frac{\partial p}{\partial s} \tag{3}$$

where s is the coordinate along the aerofoil surface.

DEVELOPMENT OF DYNAMIC STALL ON A FINITE WING

The unsteady surface pressure data recorded during the experimental programme can be used to provide a qualitative description of the dynamic stall process as a rectangular wing is pitched from 0° to 40° degrees at low Mach number, (Coton F. N *et al.* 1988). The general process is shown schematically in Fig. 2 and is outlined below. It should be noted that the detail of the process is very complicated and involves a fascinating evolution of inter-connected regions of vorticity on the wing. Figs. 2(a.b.c.d) are a very simplified representation which only identifies the behaviour of the dynamic stall and tip vortices.

Initially, the dynamic stall vortex is formed almost uniformly along the span near the quarter chord. Once formed the vortex continues to grow giving rise to increased suction near the leading edge. The uniformity of the vortex growth is short-lived and, as soon as trailing edge separation begins on the wing, the vortex system starts to exhibit strong three dimensional features. In particular, the segments of the vortex near the mid-span become stronger than those on outboard sections. The vortex system then starts to convect, moving faster at the mid-span than on outboard locations. At the same time, the weaker segments of the vortex near the tip are forced downwards toward the surface by the tip vortices and the central section of the vortex lifts from the surface, thus forming the so-called "Omega" structure. The subsequent convection of the vortex system is very complex with differential convection rates across the span. Ultimately, however, the vortex system passes the trailing edge uniformly.

Clearly, three-dimensional flows over wings are significantly more complicated than two dimensional flows over aerofoils, but the above brief description illustrates that the

vortex initiation and development exhibits typical two-dimensional features. The strong three dimensional effects on the wing begin only after trailing edge separation becomes significant. This suggests that a 2-D analysis at each span location would be sufficient to detect vortex inception. All results shown in this work have been obtained from a two-dimensional analysis of vorticity flux.

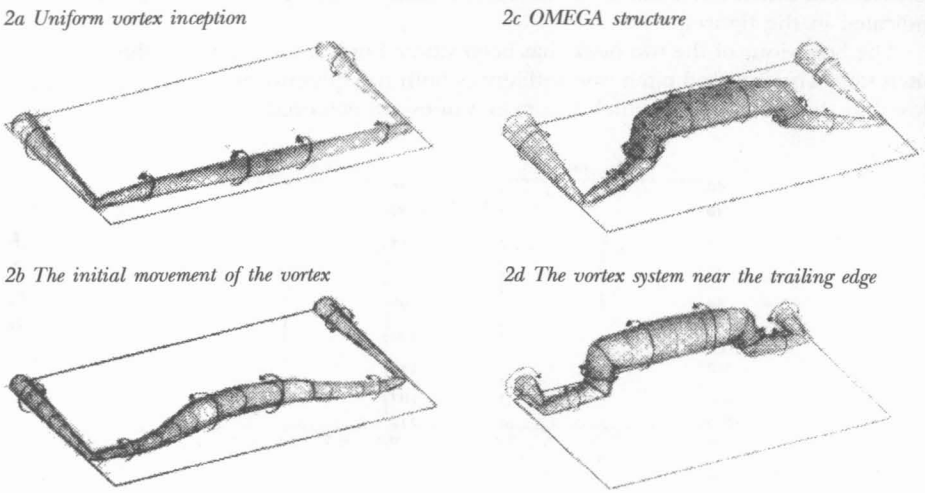

Fig. 2. Vortex system on rectangular wing in pitching Motion

ANALYSIS AND RESULTS

On the basis of Eqn. (3), it was possible to determine the chordal distribution of vorticity flux at each of six spanwise positions on the test wing. Fig. 3 presents this information for an incidence of 27.8 degrees during a ramp test at a reduced pitch rate of 0.01. In the figure, the value of the surface ordinate is zero at the upper surface trailing edge and increases with distance along the surface, reaching a maximum at the lower surface trailing edge. From the figure, it is clear that the basic form of the vorticity flux distribution is the same regardless of the spanwise location on the wing. In all cases the vorticity is introduced into the flow primarily from a region of the surface in the neighbourhood of the leading edge; within the first 3% of the chord. The bulk of this vorticity flux is, at high incidence, concentrated in two main bipolar peaks: S^+ and S^-, where S^+ is a sink of vorticity on the upper surface and S^- is a source of vorticity on the lower surface behind the stagnation point. The value of the peak S^- decreases as the aerofoil pitches up, reaches a minimum negative value when the dynamic stall vortex is formed and then increases rapidly. In the meantime, the peak S^+ continues to increase, feeding the dynamic stall vortex and reaches a maximum value much later. Consequently, the vorticity sink S^+ appears to be responsible for most of vorticity that is channelled in to the dynamic stall vortex.

These changes in the peak values are more clearly illustrated in Fig. 4 which shows the variation of the chordal distribution of vorticity flux with incidence at 57% of span. In fact, this figure shows that, if the early stages of the ramp motion are also considered, there are actually three distinct peaks in the vorticity flux distribution. The ridge labelled as "peak 1" in the first part of the diagram is a source of positive vorticity which is located on the lower surface and moves in the same direction as the stagnation point

as the incidence increases. As it moves, however, it gradually decreases in strength and is replaced on the upper surface by "peak 2" that corresponds to S^+ identified above. During this process, the ridge identified in the figure as "peak 3" on the lower surface, and corresponding to S^-, steadily grows in strength before reaching a minimum when the growth of the dynamic stall vortex is initiated. The local effect of this vortex on the vorticity flux distribution can be observed as a disturbance in the vicinity of "peak 2" as indicated in the figure.

The behaviour of the two peaks has been studied over a wide range of dimensionless pitch rate. The reduced pitch rate influences both the quantity of vorticity entering the flow and the incidence at which the peak values are achieved.

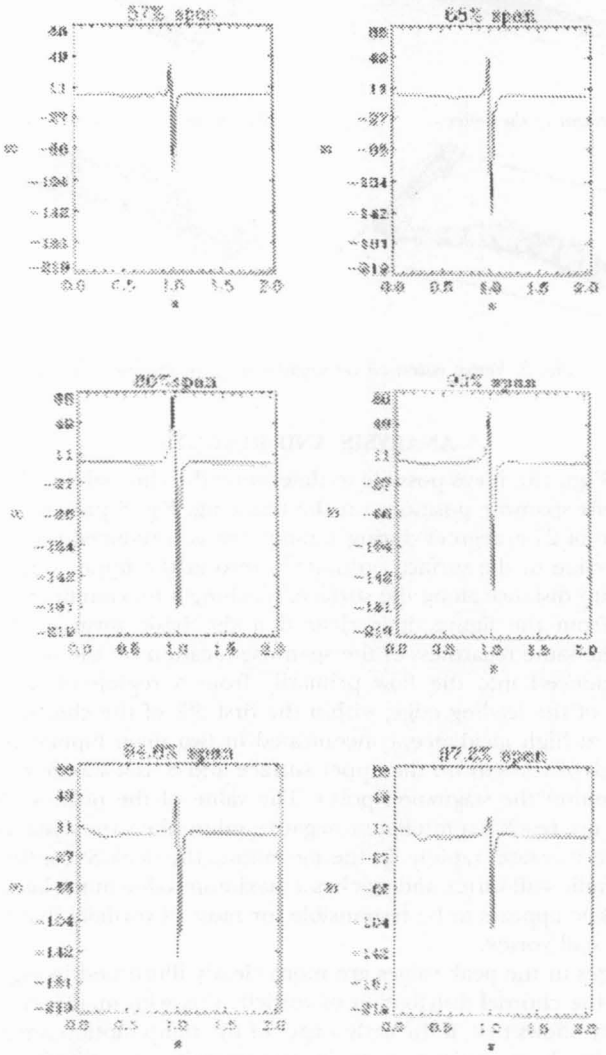

Fig. 3. Vorticity flux at reduced pitch rate 0.01 and angle of incidence 27.8 at six span location

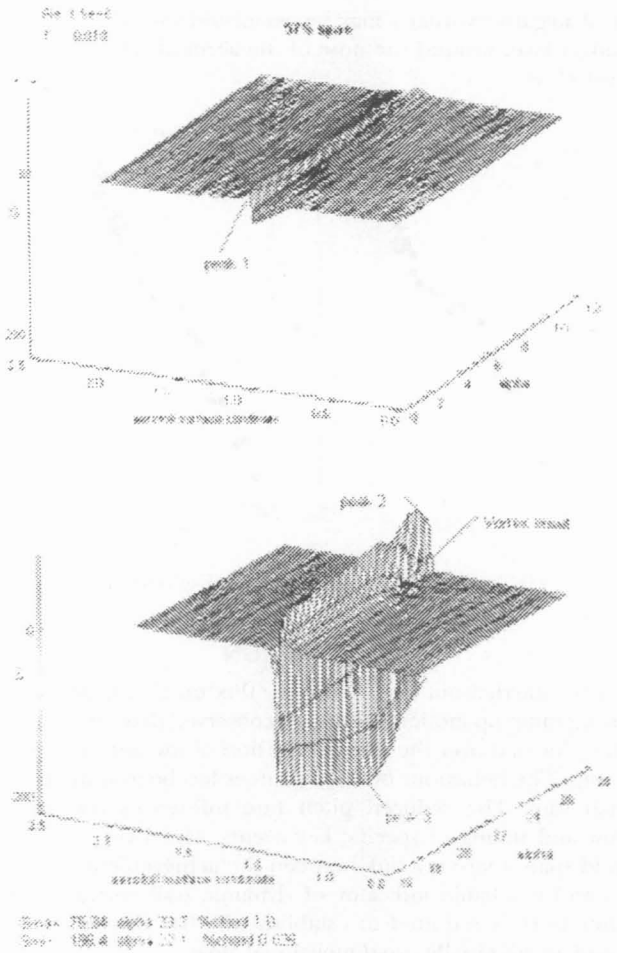

Fig. 4. Chordwise S distribution against incidence at 57% span and red. pitch rate 0.01

CP DEVIATION AND VORTICITY FLUX

It is likely that location of the vorticity sources near the leading edge and their growth and decay will, in some way, be linked to the formation of the dynamic stall vortex and its subsequent rearwards motion. It had already been established (Rosenhead 1963) that Cp deviation is a reliable indicator of dynamic stall vortex formation and so it was appropriate to examine the relationship between this and vorticity flux. Fig. 5 shows the variation of the incidence of Cp deviation at two span stations with reduced pitch rate. In each case, the chordal position used is that where Cp deviation occurred first. Also shown in the figure is the corresponding variation of the incidence at which the minimum value of S -occurred. In each case, the level of agreement between the two events is very good suggesting that the minimum in S - is a reliable indicator of vortex inception. One possible explanation of this link between dynamic stall vortex onset and

the production of negative vorticity may be associated with the balance of vorticity in/out of the boundary layer around the nose of the aerofoil. The exact mechanism of this process is not yet clear.

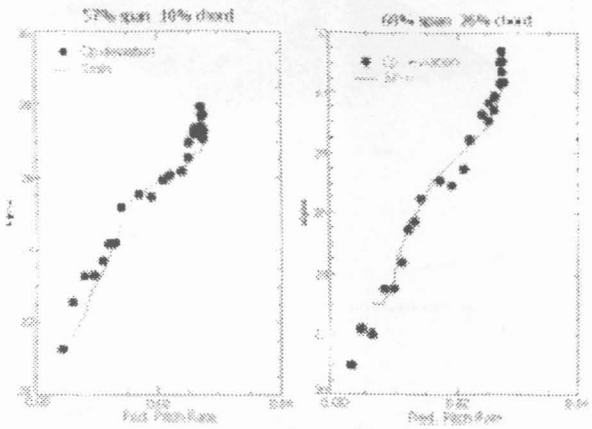

Fig. 5. Cp deviation and negative peak of vorticity flux

CONCLUSION

An analysis has been carried out of the vorticity flux on a wing model with NACA 0015 cross-section during ramp-up motion. It has been observed that there are two concentrated sources of vorticity located over the forward portion of the aerofoil surface at each span station on the wing. The behaviour of these sources has been studied over a large range of reduced pitch rate. The reduced pitch rate influences the quantity of vorticity entering the flow and timing of specific key events. Moreover, it has been established that, near the mid span, there is a link between the achievement of the minimum value of vorticity flux and a reliable indicator of dynamic stall vortex formation called Cp deviation. Further work is required to establish whether this relationship holds at all span locations and in nominally two-dimensional flow.

NOTATION

ν Viscosity
ω_z Spanwise mean vorticity
α Incidence
$\dot{\alpha}$ Instantaneous pitch rate
v Translation velocity
s Aerofoil surface ordinate measured anticlockwise from the trailing edge
x Coordinate along the surface
y Normal to the surface
c Model chord
r Reduced pitch rate ($\dot{\alpha}c/2U$)
U Freestream speed
U_s Surface tangential speed
V Transpiration velocity

S Vorticity Flux
S^+ Positive peak of vorticity flux
S^- Negative peak of vorticity flux

ACKNOWLEDGEMENT

This work was sponsored by the U.K Department of Trade and Industry under Research Agreement ASF/3221U with D.E.R.A Farnborough.

REFERENCES

CARR L.W., MCALISTER K.W. and MCCROSKEY W.J. Analysis of the development of dynamic stall based on oscillating airfoil experiments. NASA TN-838, January 1977

COTON F.N, R.A.McD, D. JIANG and R.GILMOUR. An experimental study of the effect of pitch rate on the dynamic stall of a finite wing. AIAA Paper 83-2533, October, 1983.

LIGHTHILL M.J. Introduction Boundary Layer Theory.

ROSENHEAD L. 1963. Editor Laminar Boundary Layers, Oxford University Press.